

PULSE REVERSE ELECTRODEPOSITION OF SPHERICAL Ni-MWCNT COMPOSITE SKEIN

M. Attarchi*

Materials and Energy Research Center
P.O. Box 31787-316, Karaj, Iran
attarchi@gmail.com

S.K. Sadrnezhaad

Center of Excellence for Production of Advanced Materials, Department of Materials Science and Engineering
Sharif University of Technology, P.O. Box 11365-9466, Tehran, Iran
Materials and Energy Research Center, P.O. Box 14155-4777, Tehran, Iran
sadrnezh@sharif.edu

*Corresponding Author

(Received: September 24, 2007 – Accepted in Revised Form: February 19, 2009)

Abstract Watt's bath and pulse reverse (PR) electrodeposition is used to produce spherical nickel-multi wall carbon nanotubes (Ni-MWCNT) of 2.00, 0.93, 1.63 and 6.71 μm diameter and a variety of size distributions. For 60 cycles, an absolute electrodeposition current of 18 A/dm^2 is applied at current ratios of $i_{ii} = i_{\text{dissolution}}/i_{\text{deposition}} = 0, 0.077, 0.200$ and 0.368. A simple exponential equation is fitted to each pulse response by a resistance-capacitance (RC) simple model giving different time constants usable for diagnosing the effect of different parameters. Results show that PR electrodeposition is capable of producing microspherical Ni-MWCNT composite skeins of different diameters and size distributions. This could be identified with the time constant of the process.

Keywords Ni Composite, MWCNT, Spherical Skein Composite, Pulse Reverse Electrodeposition

چکیده برای تولید کره‌های کامپوزیتی نیکل-نانوتیوپ‌های چنددیواره با قطرهای متغییر (۰/۹۳، ۱/۶۳ و ۶/۷۱ میکرومتر) و توزیع اندازه متغییر از روش رسوب‌دهی پالس معکوس (PR) در حمام وات استفاده شد. شصت سیکل با مقدار جریان مطلق رسوب‌دهی ۱۸ A/dm^2 و با نسبت جریان‌های $(i_{ii} = i_{\text{dissolution}}/i_{\text{deposition}})$ صفر، ۰/۰۷۷، ۰/۲۰۰ و ۰/۳۶۸ اعمال شد. یک معادله نمایی ساده به پاسخ هر پالس با فرض مدل ساده مقاومت-خازن برای درک اثر پارامترهای مختلف پرازش شد. نتایج نشان داد رسوب‌دهی به روش PR توانایی تولید کلاف‌های کامپوزیتی Ni-MWCNT با قطر مختلف و توزیع ابعاد را دارد. این پارامترها را می‌توان با ثابت زمانی فرآیند شناسایی کرد.

1. INTRODUCTION

Nickel-base materials have desirable corrosion resistance, acceptable mechanical properties and high catalytic activity. In order to increase the catalytic power of nickel, either a porous or a roughened-surface material is used. Nickel based composites produced by an electrochemical method are utilizable for this purpose [1]. Carbon nanotubes (CNTs) of large elastic moduli and high electrical conductivities are appropriate candidates for making high power catalysts [2-6].

The interaction between CNT and different metals

has been studied before [7]. Various researchers have produced metal-CNT samples through different electroplating and electroless deposition methods discussed in the literature [2,4-6,8]. These electrochemical methods have a lower impact on the environment than the high temperature methods. Pulse reverse electrodeposition method is an electrochemical procedure devised for improvement of various coating properties like corrosion resistance and electrocatalytic effects [1,9]. This method has recently been applied to produce composite coatings of special interest [10-14]. Kollia and Spyrellis [15,16] have, for example, discussed relationship

between texture, roughness and microhardness of the nickel layers electrodeposited using different PR electrodeposition parameters. Pulse electrodeposition process has also been used to produce ultra-fine-grained nickel coatings of preferred crystallographic orientations, Ni nanowire and Ni/Fe nanocrystalline objects [17-20]. A Ni-CNT composite has also been produced by electrodeposition method by Dai, et al [21] and Jin, et al [22]. These researchers have also studied the corrosion resistance, mechanical properties, wear resistance and electrocatalytic behavior of the produced composite layers [21,22].

The electrodeposition process can lead to two distinct morphologies: (1) nanospherical metallic CNTs and (b) CNTs coated with a metallic layer [2,4]. This article discusses the results obtained by using the PR electrodeposition method for production of a novel microspherical Ni-MWCNT composite of skein-like morphology having a carefully controlled radius as well as a required particle size distribution.

2. MATERIALS AND METHODS

A Watt's bath containing 300 gr/lit $\text{NiSO}_4 \cdot 6\text{H}_2\text{O}$, 45 gr/lit $\text{NiCl}_2 \cdot 6\text{H}_2\text{O}$ and 40 gr/lit H_3BO_3 with a pH adjusted at 5.0 and a triple electrode cell were used to run the pulse reverse electrodeposition tests of this research. MWCNT (>95 wt % purity) with a concentration of 2 gr/lit was added to the solution which was magnetically stirred for 1 hour and then ultrasonically shaken at 50°C for 12 hours. The auxiliary electrode was a long Ni spring; the reference electrode was an Ag/AgCl electrode and the working electrode was a piece of Ni wire. The working electrodes were cleaned by CH_3COCH_3 / $\text{C}_2\text{H}_5\text{OH}$ in an ultrasonic bath after abrasion to number 1000. The exposed surface of the Ni electrodes were 0.32 cm². All tests were carried out in a 100 ml standard cell beaker containing a slowly stirred solution kept at 50°C.

The PR electrodeposition tests were carried out with an Autolab[®] PGSTAT30 potentiostat. Each step consisted of 60 deposition-dissolution cycles. Each cycle took 5 seconds with no relaxation time. Four sets of current densities were employed: (a) 18 A/dm² deposition and 0 A/dm² dissolution [$i_{\text{dissolution}}/i_{\text{deposition}}=0$], (b) 19.5 A/dm² deposition

and 1.5 A/dm² dissolution [$i_{\text{dissolution}}/i_{\text{deposition}}=0.077$], (c) 22.5 A/dm² deposition and 4.5 A/dm² dissolution [$i_{\text{dissolution}}/i_{\text{deposition}}=0.200$] and (d) 28.5 A/dm² deposition and 10.5 A/dm² dissolution [$i_{\text{dissolution}}/i_{\text{deposition}}=0.368$]. During all 60 cycles, the absolute electrodeposition current was remained at 18 A/dm². After preparation, all electrodes were immersed in distilled water for 24 hours and then dried in the air. Phase identification and crystallographic investigations were carried out using X-ray diffraction analysis (XRD, Simens D500 diffractometer) with Cu-K α radiation. Morphology of the surface film was studied by scanning electron microscopy (SEM, Philips XL30).

3. RESULTS

SEM images of the working electrodes produced at different current ratios are shown in Figure 1. Spherical Ni-MWCNT composites of different diameters are observable in the figure. Particle radii and size distribution can both be estimated from SEM images with X5000 magnification. Another part of the surface of the electrodes which doesn't show any clustering of Ni-MWCNT composite is shown in Figures 2. A schematic scheme of the proposed mechanism is illustrated in Figure 3. XRD micrographs of synthesized nanocomposites are depicted in Figure 4. Deposition parts of the potential-time curve that gained from PR electrodeposition with RC simple model assumption [23] were fitted into an exponential equation of the type: $a \times \exp(-t/\tau) + b$. The time constants (τ) were obtained against deposition-dissolution cycle number as shown in Figure 5.

4. DISCUSSION

Prior to deposition, nickel ions and MWCNTs are flown in the solution to adsorb on the surface of the electrode. When current is applied for deposition, Ni ions are reduced and MWCNTs nearest to the surface are engulfed at earlier steps. Engulfed and connected MWCNTs let the current to pass very well and produce needle like branches connected to the surface. Tips and surfaces of MWCNTs are good places for nucleation of nickel.

A relatively high current density is used in this study to immediately cause reduction of nickel and production of CNT with a Ni cover. High current densities generally lead to rough and powdery deposits in direct plating as well as in the composite coating process [24-26]. In conventional electroplating, new nuclei prefer high energy sites (such as defects) for growth [26,27]. Earlier nucleation covers, hence, the surface with a large number of nuclei. In pulse electrodeposition, new nuclei can similarly be generated earlier resulting in a lower grain size than that obtained in direct electrodeposition. Spherical morphology of Ni-MWCNT means that when the same site locates at different places, it can act as a preferred nucleation site with a high current density that prevents smooth surface formation. In the PR process, the dissolution step comes right after the deposition step. When dissolution occurs, a high energy site becomes preferable for further dissolution. Sharp sites, boundaries and high energy crystallographic planes and directions will first dissolve. Formation of different interfacial inhibitors such as nickel hydroxide, adsorbed hydrogen, hydrogen gas and organic compounds is also encouraged at some preferred directions [15-17].

Figure 1 shows spherical Ni-MWCNT composites of skein-like morphology with different radii. The mean diameter of the spheres are 2.00, 0.93, 1.63 and 6.71 μm with standard deviations of 0.37 (18%), 0.17 (18%), 0.49 (30%) and 2.11 (25%) corresponding respectively to the current ratios of 0, 0.077, 0.200 and 0.368. Radii of the spheres are reduced from sample a to sample b, but they are increased from sample b to samples c and d. A minimum radius is obtained at condition b (current density of 19.5 A/dm^2 for deposition and 1.5 A/dm^2 for dissolution). Maximum radius is gained at condition d which have a current density of 28.5 A/dm^2 for deposition and 10.5 A/dm^2 for dissolution. Samples a and c have similar radius but their size distribution is not the same. Sample c has an extended radius distribution. At these conditions, spherical morphology means high number of nucleation sites in electrodeposition and dissolution at high energy sites such as spherical contact regions. Dissolution of Ni-MWCNT composite causes remaining of MWCNTs at the outer surface regions.

With mere electrodeposition step corresponding

to Figure 1a, the current density has been sufficient for sphere production. At a short period of time, high electrodeposition current density causes reduction of mobility of Ni ions at the surface while the surface nucleation sites increases. Ni merely covers the CNTs when electrodeposition current doesn't suffice coating of nickel-CNT composite. CNTs embed in Ni matrix when electrodeposition current is too high [3,26,27]. A number of Ni-MWCNT clusters are seen in Figure 1a that can act as appropriate nucleation sites. These clusters are different from the composites grown with the spherical shape. The spheres shown in Figure 1b are smaller than those shown in the other figures. It seems that 1.5 A/dm^2 dissolution current density after 19.5 A/dm^2 deposition current density can produce same homogeneous nucleation sites for growth and reduction of the spheres diameters. Differentiation between nucleation sites and grown spheres is difficult at this stage because dissolution process can also produce new nucleation sites. In the third procedure corresponding to the morphology shown in Figure 1c, steady state conditions are changed to inhomogeneous sphere nucleation. The remaining rough clusters of Ni-MWCNT act here as nucleation sites during deposition step and Ni ions reduce simultaneously as engulfed MWCNT deposit. The dissolution step remains near steady state nucleation. At 4th procedure that corresponds to the morphology shown in Figure 1d, the radii of the spheres increase. Electrodeposition rapidly happens while as a result of high current density in the dissolution step; week spheres (and nuclei) dissolve and large spheres of higher stability remain.

Cluster free parts of the surfaces are shown in Figure 2. MWCNTs engulfed in Ni matrix with disperse nucleation sites are only seen in the electrode surfaces of procedures a and b shown in Figures 2a and 2b. This behavior confirms a good size distribution of the spherical particles. Figures 2c and 2d illustrate, however, that at higher deposition current densities, a network of rough MWCNT-Ni composite clusters is formed. A higher dissolution current density causes CNTs of Figure 2d to be barer than that of Figure 2c. Figure 3 demonstrates the proposed mechanism of the electrodeposition process.

XRD patterns are illustrated in Figure 4. These

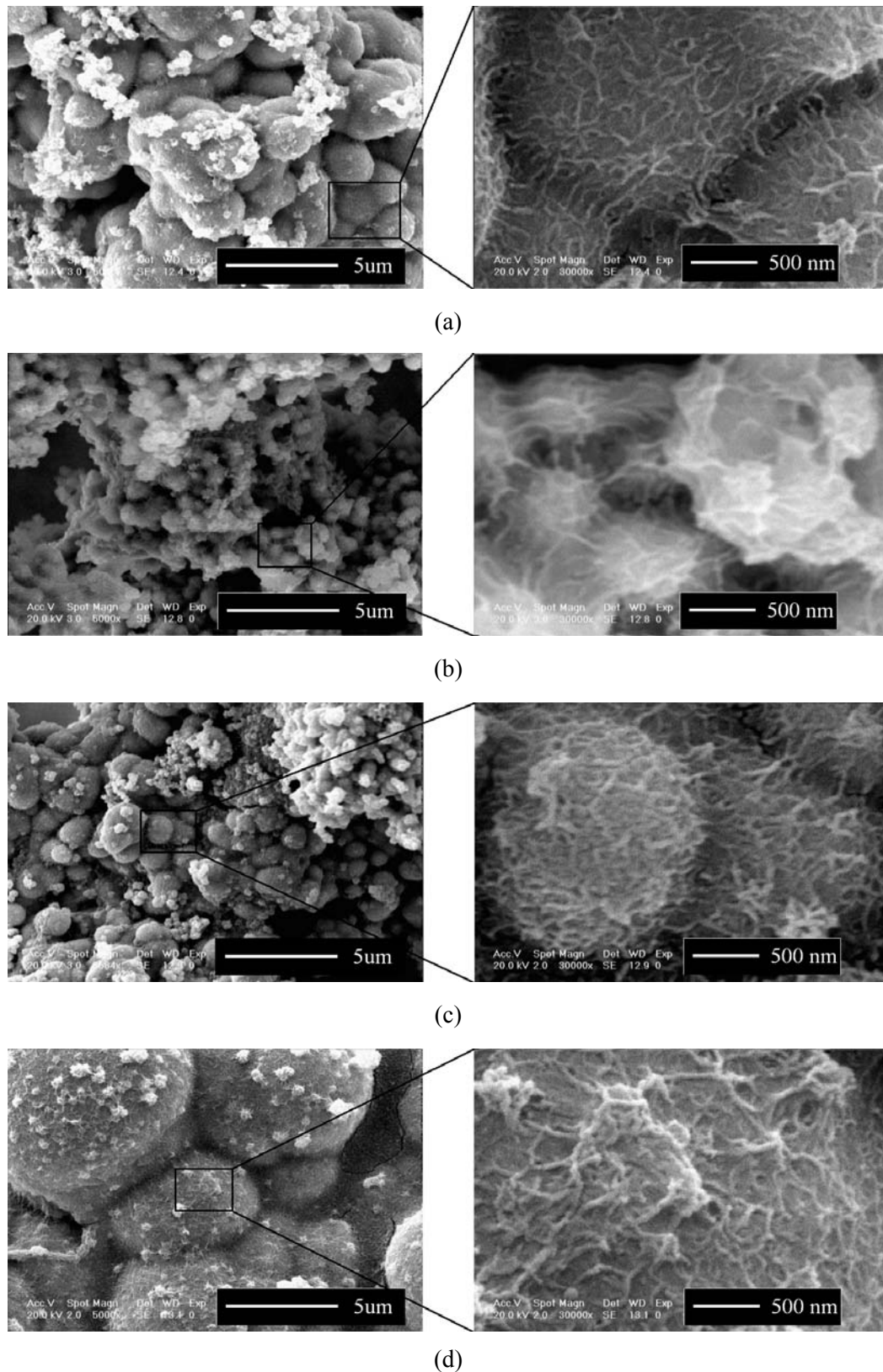
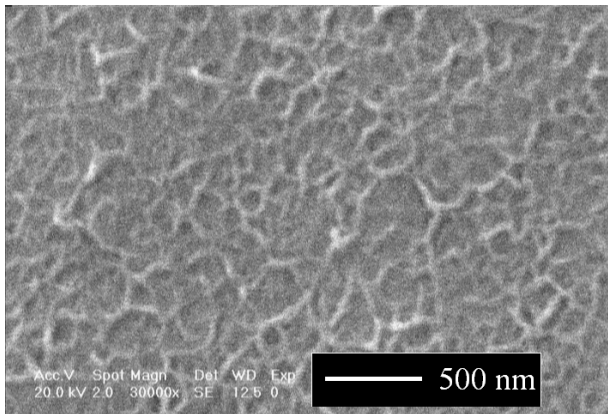
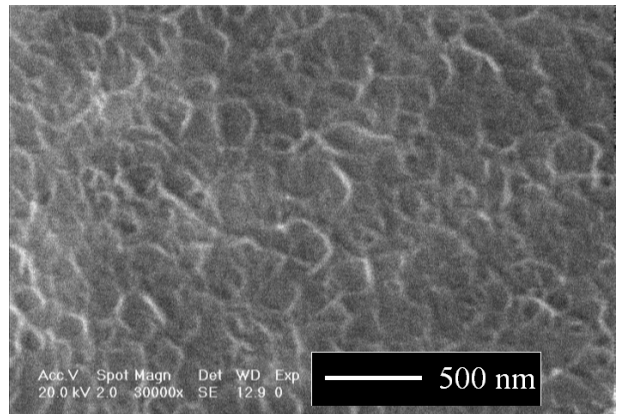


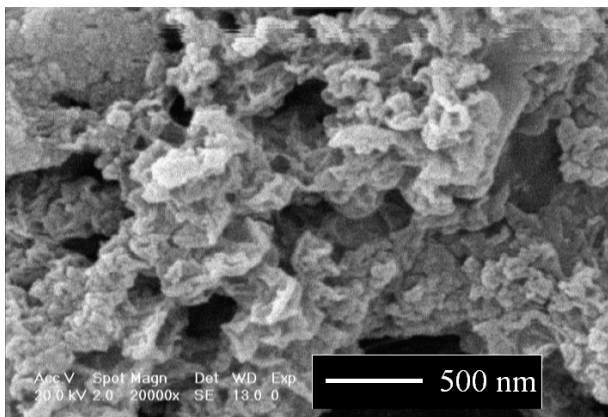
Figure 1. SEM images of the sample surfaces produced at (a) $ii = 0$, (b) $ii = 0.077$, (c) $ii = 0.200$ and (d) $ii = 0.368$.



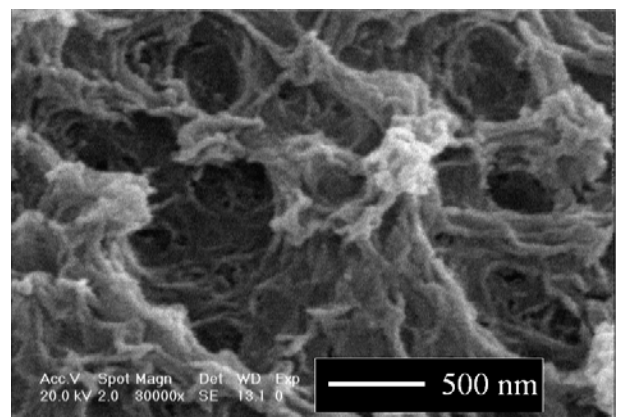
(a)



(b)



(c)



(d)

Figure 2. SEM images of the non-clustered electrode surfaces produced at (a) $ii = 0$, (b) $ii = 0.077$, (c) $ii = 0.200$ and (d) $ii = 0.368$.

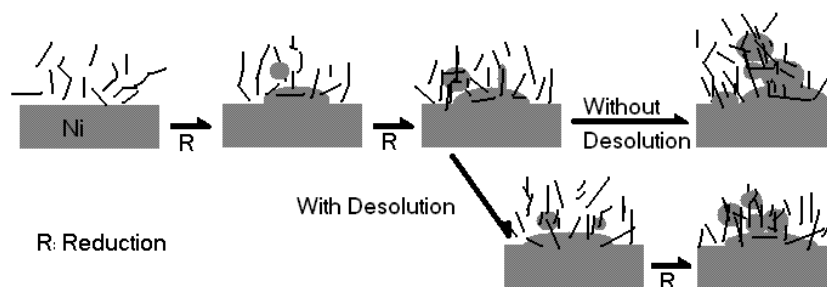


Figure 3. Schematic scheme of pulse reverse electrodeposition of Ni-MWCNT mechanism.

patterns are confirmed Ni-MWCNT structure. Ni crystallographic face were not change sharply by different pulse reverse electrodeposition which

used in the presence study.

Time constant versus cycle for deposition for PR electrodeposition process is depicted in Figure 5

for all four procedures. Based on a simple RC circuit, the time constant of the impulse response to current excitation is defined as $\tau = RC$ in which C is the capacitance and R is the resistance of the circuit. For the exponential function $a \cdot \exp(-t/\tau) + b$, a higher value of τ means a slower speed than the system with a lower time constant.

As shown in Figure 5, during the first procedure that the dissolution process doesn't exist, the time

constant of the process increases continuously until it reaches to a rather constant value after the 30th cycle. This means that the speed of electrodeposition decreases with time. Referring to Figure 1a, one can conclude that the reduction of speed is as result of the increase of the surface which causes the increase of the capacitance and the reduction of the specific current densities. These parameters can in fact reach to a steady

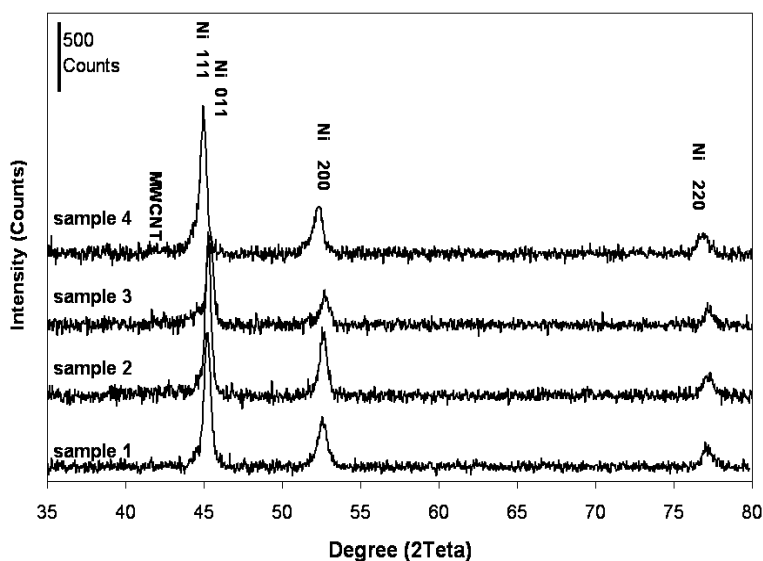


Figure 4. XRD Patterns of Ni-MWCNTs samples produced at (a) $ii = 0$, (b) $ii = 0.077$, (c) $ii = 0.200$ and (d) $ii = 0.368$.

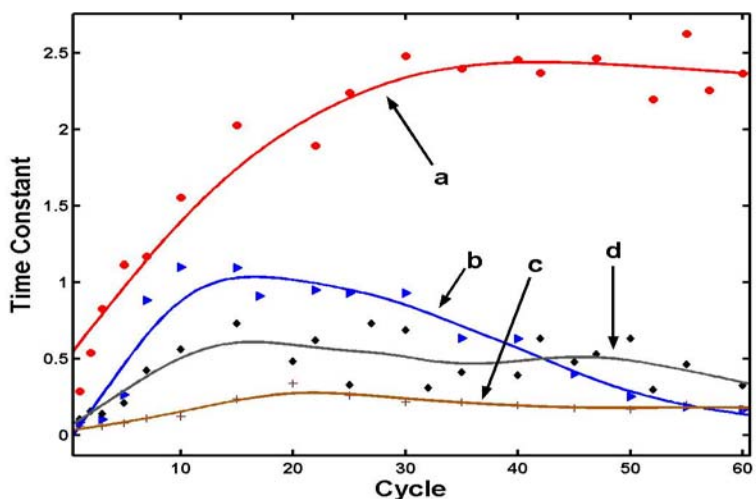


Figure 5. Effect of deposition-dissolution cycling on time constants obtained from PR electrodeposition current control) response for (a) $ii = 0$, (b) $ii = 0.077$, (c) $ii = 0.200$ and (d) $ii = 0.368$.

value in absence of the dissolution current. In case b, the time constant firstly increases with time and then gradually decreases to a lower value. The first increase can be referred to the surface increase which causes increasing of the capacitance and/or decreasing of the current density in the surface. Supposing that the speed of the structural growth reaches to a steady state, reduction of time-constant in the second stage as well as the increasing of the electrodeposition rate both indicate a greater number of active nucleation sites as compared to the first step. The structural growth of this step seems therefore resulting from the greater number of active nucleation sites rather than the increasing of the surface area which may even decrease.

The time constant for the 3rd procedure is lower than that for all other procedures. In the first part of this study, inhomogeneous sphere diameters are considered. By elapsing of the time, the surface area increases by composite cluster formation. Under these conditions, different sizes of the spheres and the nucleation sites appear. By proceeding of the procedure, if new nucleation sites appear and the growth rate becomes proportionate to the enlargement of the surface, the rate of the surface phenomenon must remain a large constant. In the latest case which has a higher spherical radius, time constant slowly increases to a constant value for the remaining cycle. Because of the relatively large radii of the spheres (limited activated nucleation sites) and growth of composite clusters (increase in surface area), one can conclude that surface enlargement is proportional to the current densities at the surface.

Without dissolution, time constant increases in general up to a certain value. Lowest particle radius is obtained by first increasing and then decreasing of the time constant. A higher radius reaches when a lower increasing of the time constant firstly occurs and then it retains at a fixed value. Inhomogeneous structure is produced at the lowest time constant which corresponds to a fast surface phenomenon.

5. CONCLUSIOS

By using PR electrodeposition, microspherical Ni-MWCNT composite skeins are obtained. Variation of the current ratio $i_i = i_{\text{dissolution}}/i_{\text{deposition}}$ causes the

diameter and distribution of the spheres to change. A large i_i value results in increasing of the spheres diameter and the surface roughness. Time-constant analysis has given simple rules for prediction of the spheres diameters and their size distribution.

6. REFERENCES

1. Panek, J. and Budniok, A., "Production and Electrochemical Characterization of Ni-Base Composite Coatings Containing Titanium, Vanadium or Molybdenum Powders", *Surface and Coatings Technology*, Vol. 201, (2007), 6478-83.
2. Arai, S., Endo, M. and Kaneko, N., "Ni-Deposited Multi-Walled Carbon Nanotubes by Electrodeposition", *Carbon*, Vol. 42, (2004), 641-644.
3. Guo, C., Zuo, Y., Zhao, X., Zhao, J. and Xiong, J., "The Effects of Pulse-Reverse Parameters on the Properties of Ni-Carbon Nanotubes Composite Coatings", *Surface and Coatings Technology*, Vol. 201, (2007), 9491-9496.
4. Wang, F., Arai, S. and Endo, M., "Preparation of Nickel-Carbon Nanofiber Composites by a Pulse-Reverse Electrodeposition Process", *Electrochemistry Communications*, Vol. 7, (2005), 674-678.
5. Arai, S. and Endo, M., "Carbon Nanofiber Composite Powder Prepared by Electrodeposition", *Electrochemistry Communications*, Vol. 5, (2003), 797-799.
6. Arai, S. and Endo, M., "Various Carbon Nanofiber-Copper Composites Films Prepared by Electrodeposition", *Electrochemistry Communications*, Vol. 7, (2005), 19-22.
7. Zhang, Y., Franklin, N.W., Chen, R.J. and Dai, H., "Metal Coating Suspended Carbon Nanotubes and its Implication to Metal-Tube Interaction", *Chemical Physics Letters*, Vol. 331, (2000), 35-41.
8. Wang, F., Arai, S. and Endo, M., "The Preparation of Multi-Walled Carbon Nanotubes with a Ni-P Coating by an Electroless Deposition Process", *Carbon*, Vol. 43, (2005), 1716-1721.
9. Chen, X.H., Chen, C.S., Xiao, H.N., Cheng, F.Q., Zhang, G. and Yi, G.J., "Corrosion Behavior of Carbon Nanotubes-Ni Composite Coating", *Surface and Coatings Technology*, Vol. 191, (2005), 351-356.
10. Fenineche, N., El-Kedim, O. and Coddet, C., "The Effect of Plus Parameters on the Electrodeposition of Co-Ni Alloys", *Surface and Coatings Technology*, Vol. 48, (1991), 205-209.
11. Sorkhabi, H.A., Hagrah, H., Ahmadi, N.P. and Manzoori, J., "Zinc-Nickel Alloy Coatings Electrodeposited from a Chloride Bath Using Direct and Pulse Current", *Surface and Coatings Technology*, Vol. 140, (2001), 278-283.
12. Chang, L.M., An, M.Z., Gue, H.F. and Shi, S.Y., "Microstructure and Properties of Ni-Co/Nano-Al₂O₃ Composite Coatings by Pulse Reversal Current Electrodeposition", *Applied Surface Science*, Vol. 253, (2006), 2132-2137.

13. Li, Y., Jiang, H., Pang, L., Wang, B. and Liang, X., "Novel Application of Nanocrystalline Nickel Electrodeposit: Making Good Diamond Tools Easily, Efficiency and Economically", *Surface and Coatings Technology*, Vol. 201, (2007), 5925-5930.
14. Marlot, A., Kern, P. and Landolt, D., "Pulse Plating of Ni-Mo Alloys from Ni-Rich Electrolytes", *Electrochimica Acta*, Vol. 48, (2002), 29-36.
15. Kollia, C. and Spyrellis, N., "Textural Modification in Nickel Electrodeposition under Pulse Reversed Current", *Surface Coatings Technology*, Vol. 57, (1993), 71-75.
16. Kollia, C. and Spyrellis, N., "Microhardness and Roughness in Nickel Electrodeposition Under Pulse Reversed Current Conditions", *Surface and Coatings Technology*, Vol. 57, (1993), 101-105.
17. El-Sherik, A.M., Erb, U. and Page, J., "Microstructural Evaluation in Pulse Plated Nickel Electrodeposits", *Surface and Coatings Technology*, Vol. 88, (1996), 70-78.
18. Seet, H.L., Li, X.P., Ng, W.C., Chia, H.Y., Zheng, H.M. and Lee, K.S., "Development of Ni₈₀Fe₂₀/Cu Nanocrystalline Composite Wires by Pulse-Reverse Electrodeposition", *Journal of Alloys and Compounds*, Vol. 449, (2008), 279-283.
19. Nielsch, K., Muller, F., Li, A. and Gosele, U., "Uniform Nickel Deposition into Ordered Aluminium Pores by Pulsed Electrodeposition", *Advanced Materials*, Vol. 12, (2000), 582-586.
20. Zhang, Y., Li, G., Wu, Y., Zhang, B., Song, W. and Zhang, L., "Antimony Nanowire Arrays Fabricated by Pulsed Electrodeposition in Anodic Alumina Membranes", *Advanced Materials*, Vol. 14, (2002), 1227-1230.
21. Dai, P.Q., Xu, W.C. and Huang, Q.Y., "Mechanical Properties and Microstructure of Nanocrystalline Nickel-Carbon Nanotube Composite Produced by Electrodeposition", *Materials Science and Engineering A*, Vol. 483, (2007), 172-174.
22. Jin, G.P., Ding, Y.F. and Zheng, P.P., "Electrodeposition of Nickel Nanoparticles on Functional MWCNT Surfaces for Ethanol Oxidation", *Journal of Power Sources*, Vol. 166, (2007), 80-86.
23. Gladstein, M. and Guterman, H., "A New Approach to Controlling Metal Deposition During the Pulse Plating Process", *Metal Finishing*, (2002), 26-33.
24. Zimmerman, A.F., Clark, D.G., Aust, K.T. and Erb, U., "Pulse Electrodeposition of Ni-SiC Nanocomposite", *Materials Letters*, Vol. 52, (2002), 85-90.
25. Magdy, A.M.I., "Black Nickel Electrodeposition from a Modified Watts Bath", *Journal of Applied Electrochemistry*, Vol. 36, (2006), 295-301.
26. Guo, C., Zuo, Y., Zhao, X., Zhao, J. and Xiong, J., "The Effects of Electrodeposition Current Density on Properties of Ni-CNTs Composite Coatings", *Surface and Coatings Technology*, Vol. 202, (2008), 3246-3250.
27. Lampke, T., Wielage, B., Dietrich, D. and Leopold, A., "Details of Crystalline Growth in Co-Deposited Electroplated Nickel Films with Hard (Nano)Particles", *Applied Surface Science*, Vol. 253, (2006), 2399-2408.